9th Biennial International Conference
& Exposition on Petroleum Geophysics

"HYDERABAD 2012"

P-440

# Tomographic imaging of the Gondwana sediments and shallow Basement configuration for hydrocarbon potential in the Mahanadi delta, India

***Laxmidhar Behera*, and Dipankar Sarkar,*** *NGRI*

***Summary***

*A tomographic P-wave velocity image of the shallow basement structure is derived using first-arrival seismic data along the 120 km E-W trending seismic profile in the Mahanadi delta, India. The tomographic image depicts smooth velocity variations of Quaternary (1.8-2.0 km/s) and Gondwana sediments (3.5-4.5 km/s) lying above the basement (5.9-6.1 km/s). The basement is high ly distorted due to the presence of deep basinal faults, which reach maximum 6.0 km depth forming the Cuttack depression (Gondwana graben) in which thick (3.0 km) column of Gondwana sediments were deposited. These Early Cretaceous Gondwana sediements can be considered as hydrocarbon bearing having excellent trapping mechanism because of the presence of high velocity basalts interlaced and sandwiched between two sequences of the Gondwana sediments within the Cuttack depression. The basement is uplifted on either side of the depression/graben forming Chandikhol ridge in the west and Bhubaneswar ridge in the east of the profile with anomalous high-velocity (5.5 km/s) dyke intrusions imaged beneath the flanks of the graben and presence of thick (>2.0 km) magmatic intrusives (6.5 km/s) lying below the basement. These features are favorable for providing sufficient cooking condition for the generation and maturation of hydrocarbon in the Mahanadi delta, which may find significant potential for hydrocarbon exploration in which several exploratory wells drilled show the presence of hydrocarbon in the delta.*

## Introduction

The Mahanadi delta of Orissa is an important deltaic sedimentary basin of east-coast India due to the evolution, complex geology and tectonic setting (Figure 1). The delta was formed due to several stages of rifting, subsidence, followed by sediment deposition and uplift because of tensional forces during the Late Jurassic (Sastri et al., 1974). The Mahanadi delta and Lambert graben of Antarctica were conjugate with each other before breakup of the Indian Plate with East-Gondwana (Fedorov et al., 1982). After breakup, both Mahanadi delta and Lambert graben were effected by large scale Early Cretaceous volcanism. On the basis of available seismic, gravity, aeromagnetic, heat flow, and geological information, many geoscientists prefer a rift-related evolution of the Mahanadi basin. The basin was formed either as a single rift valley with syn-sedimentation and post-sedimentation faulting episodes or as a multiple rift system or it was combined with the Lambert graben in the Indo-Antarctic rift (Fedorov et al., 1982; Hofmann, 1996). This later model, that of a common intra-Gondwana rift system, is supported by many paleontologic, stratigraphic, and structural observations (Fedorov et al., 1982), which can be considered as the main basis for many recent Gondwana reconstructions. The delta also bears sign ificance because of its h ydrocarbon potential. The major shallow and deep crustal tectonic elements imaged in the delta by ray-trace modeling of first-arrival seismic refraction and wide-angle reflection data are alternate horsts and grabens along with sign ificant underplating and Moho upwarping (Behera, 2003; Behera et al., 2004). The basement highs or horsts present in the delta are called Chandikhol ridge and Bhubaneswar ridge, which surrounds the Cuttack depression called the Gondwana graben having thick Gondwana sediments. These Gondwana sediments are also exposed in some parts of the delta.

The ray-trace model using first-arrival seismic refraction data depicts a layered model with different velocities and thicknesses (Behera, 2003). The constraints on the velocity and interface structures derived by the ray-trace technique are inherently limited due to model non-uniqueness and non-linearity of the traveltime inversion problem. Hence, number of subjective approaches are employed to minimize the non-uniqueness and deal with the non-linearity by

*National Geophysical Research Institute (NGRI, CSIR), Uppal Road, Hyderabad-500007, India,*
*email: laxmidhar@ngri.res.in*

dividing the model into multiple layers and assigning a refracted phase for each layer during forward modeling, using well informations to constrain thickness of alternate volcanics and intra-trappean Gondwana sediments, adding information of local geology and Bouguer gravity data to increase the model constraint. The final model derived by this approach may be considered as geologically reasonable after several iterations without attaining velocity and structural smoothness.

On the other hand a smooth and geologically plausible model can be sought by using the same first-arrival traveltimes with the help of tomograph ic approach (Hole, 1992; Zelt and Barton, 1998) utilizing a uniform fine-grid model parameterization, which is widely used for imaging shallow sedimentary structures and deep crustal studies. Tomographic imaging is a powerful tool to visualize subsurface structures with smoother vertical velocity variations as compared to the ray-trace modeling approach. The tomograph ic inversion takes into account fitting of the data in a series of linearized iterations having a simple starting model. Also the first-arrival picks need not be classified according to the layer geometry. Here, we use the tomographic approach with a simple starting model to image the sedimentary basin with basement and sub-basement structures in the Mahanadi delta along the 120 km E-W trending Baliamba-Jagannathpur deep-seismic profile (Figure 1). The main objective of th is study is to derive a comprehensive tectonic model depicting smooth lateral and vertical velocity variations, image complex faults with horst and graben structures with suitable trapping mechanism for plausible hydrocarbon accumulation within the Gondwana sediments of the delta.

## Geology and tectonic setting

The Mahanadi basin at the eastern margin of India is arcuate in shape w ith an onshore part (Mahanadi delta) that extends from longitudes 85°E to 87°E and latitudes 19.5°N to 21°N and has a complex geological setup (Figure 1). Most of the area in the delta is covered with recent alluvium with few places having exposed Archean/Precambrian igneous and metamorphic rocks of the Eastern Ghat orogeney towards the northwest. These rocks are disposed in the form of detached hillocks striking in ENE-WSW direction bordering the Mahanadi delta (Behera et al., 2004). The exposed rocks comprise mainly of Gondwana (lower Triassic to upper Carboniferous), laterites (Pliocene to Pleistocene), granites/gneisses (Archean), khondalites (Precambrian metamorphic rocks), and charnockites/anorthosites (Precambrian igneous rocks). Fuloria (1994) has suggested the presence of a Gondwana graben and reports extensive volcanism along the rift zones of the delta. Until the Jurassic, it was an intra-continental pull-apart basin and became pericratonic after the breakup of the Gondwana (Rao, 1993).

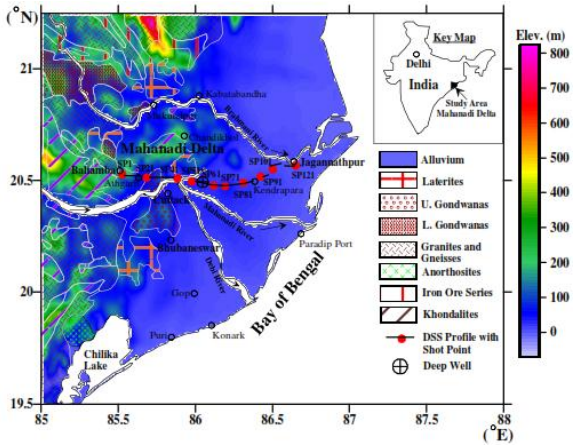


Figure 1. Geology and tectonic map of the Mahanadi delta with E-W trending Baliamba-Jagannathpur deep-seismic-sounding (DSS) profile traversing across the Mahanadi Gondwana graben between Cuttack and Kendrapara. Red dots represent s shot point (SP) locations with labels. The deep well (2993 m) drilled is marked lying on the profile. The different rocks exposed are shown along with the topography represented in color scale.

Several geophysical and geological studies have been conducted to understand geology and tectonics of the delta (Kaila et al., 1987; Mishra et al., 1999; Anand et al., 2002; Behera et al., 2002, 2004; Behera, 2003). Many wells also were drilled in the delta for hydrocarbon exploration by the oil industry (Bharali et al., 1991). The deepest well drilled (2993m) by the oil industry in the Cuttack depression shows two sequences of thin volcanic sills (100-200m) at 914m and 1861m depths, respectively (Behera et al., 2002), forming acoustic barriers to image the potential hydrocarbon bearing zones (Figure 1) with the help of conventional seismic reflection methods. The deep well cou ld not reach the basement.

## Data and methodology

### *Observed first-arrival seismic data*

The quality of first-arrival seismic refraction data along the E-W trending DSS profile in the Mahanadi delta is reasonable with good signal-to-noise (S/N) ratio. Example shot point (SP) gathers show strong P-wave refracted phases (Figure 2). The SP interval is ~10 km and average trace interval is 400-500 m after removing noisy and bad traces. First-arrival traveltimes are picked manually from the SP supergathers with an average picking uncertainties of less than 50 ms from all the 10 SP gathers. The first- arrival picks shown in Figure 2 are used to derive the basement and sub-basement configuration with the help of ray-trace modeling (Zelt and Smith, 1992). The modeled traveltimes fit the observed data within the estimated picking uncertainty of 50 ms. The detailed ray-trace model (Behera, 2003; Behera et al., 2004) along this profile shows a very shallow basement in the west called Chandikhol ridge with thin (0.3-0.5 km) cover of recent alluvium. The central part (Cuttack depression) of the profile has a deep graben (3.0 km) with 2.0 thick Gondwana sediments interlaced with two thin volcanic sequences (100-200 m) constrained from the lithology of deep well data. The graben is truncated by deep basinal faults on either side with adjacent horsts.

## Tomographic inversion method

We applied the tomographic inversion method of Zelt and Barton (1998) to the same P-wave first-arrival traveltimes picked (Figure 2) for all the SPs along the profile to estimate the total thickness and P-wave velocity (Vp) of the Early Cretaceous Gondwana sedimentary rocks above the basement along with basement and sub-basement configuration in the Mahanadi delta. The inversion method is based on the minimization of data m isfit and model roughness to provide smoothest model appropriate for data error. The synthetics traveltimes are computed by using a finite difference algorithm developed by Vidale (1988) and modified by Hole and Zelt (1995) to account for large velocity gradients during forward modeling.

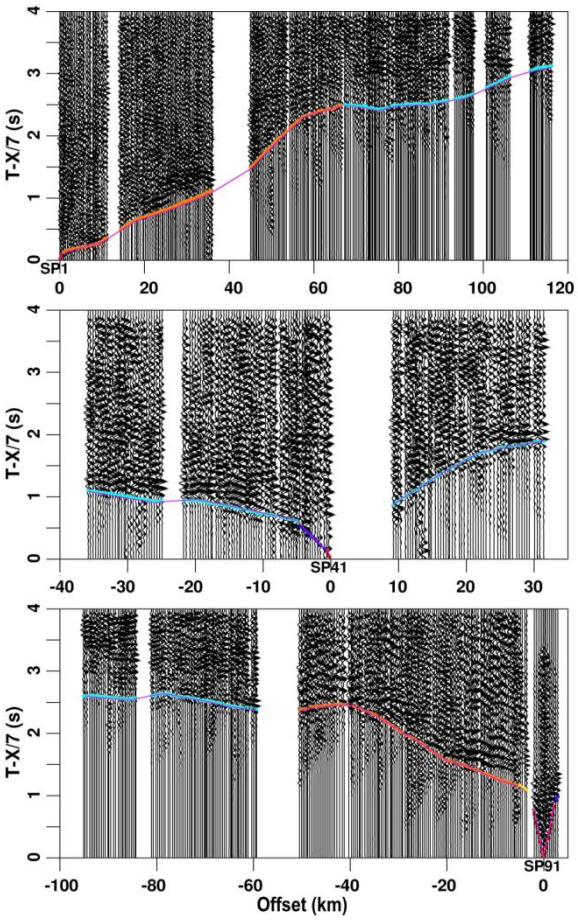


Figure 2. Three example shot gathers (SP1, SP41 and SP91) are shown with P-wave first-arrival picks (color dots corresponding to different phases of the respective layers numbers) used for ray-trace modeling. The computed responses of the ray-trace modeling are also superposed on the observed data. The data are plotted with a reduction velocity of 7.0 km/s and source receiver offsets shown along the horizontal axis in km. These traveltime picks without any phase classification are used for first-arrival traveltime tomography.

The inverse modeling formulates an objective function, which is $L_2$ norm of the combination of data error and model roughness (Lees and Crosson, 1989) and minimizes them to compute the model updates. For a model vector *m*, predicted data $d_{pre}$ and observed data $d_{obs}$ the objective function E is expressed as:

$$E(m) = \Delta d^T C_d^{-1} \Delta d + \lambda( m^T C_h^{-1} m + s_z m^T C_v^{-1} m ) \qquad (1)$$

where $\Delta d = d_{pre} - d_{obs}$ are the data errors, $C_d$ is the data covariance matrix, $C_h$ and $C_v$ are model space

covariance matrices that measure horizontal and vertical roughnesses, respectively, λ is the trade-off parameter and $s_z$ determ ines the relative importance of maintaining vertical versus horizontal model smoothness. The regularization was implemented by scalin g with inverses of data and model space covariance matrices to obtain the required smoothness of the model. To assess the quality of inversion, traveltime RMS residuals and $\chi^2$ parameters are used. Optimum values of free parameters in the inversion, which control vertical versus horizontal smoothness and model roughness were obtained from a number of runs.

Since tomographic inversion can reliably determine small perturbations in velocity field from an initial model, which represents gross features of the subsurface structure, the 1D starting $V_p$ model (Figure 3a) is constructed based on the seismic velocities obtained by Behera (2003) from ray- trace modeling. The basement was constrained to be maximum 3.1 km depth in the delta by incorporating the two sequences of thin high-velocity (5.2 km/s and 4.8 km/s) volcanics with intra-trappean Gondwana sediments (4.0 km/s and 3.8 km/s) above the basement (6.0 km/s) with the help of ray-trace modelin g of seismic refraction data (Behera, 2003; Behera et al., 2004). The ray-trace model illu strates various structural features w ith vertical velocity variations of different layers down to the basement. The 1D model derived from this ray-trace model was smoothed vertically to remove an y layering or velocity discontinuities, which may bias tomography results. The data is fit with the help of a very simple linear-gradient starting model. The zero-gradient padding from 7 to 10 km (Figure 3a) is used to prevent rays from reaching the bottom of the model. The model was defined on a uniform 0.5 km grid extending fro 0 to 120 km in the x-direction and 0-10 km in the z-direction for all forward computations. A 1.0 km lateral and 0.5 km vertical cell size was used in the inverse step, which is twice the horizontal and equal to the vertical forward node spacing, resu lting 2400 independent model parameters. A suitable cell size is one that allows the required data fit with a normalized misfit ($\chi^2$) of 1.0.

The initial trade-off parameter λ in the objective function of Eq. (1) was assigned to be 100 by trial and error so that the RMS traveltime misfit decreased by 30% after the first non-linear iteration, which indicates that the inversion is neither trapped in a local minima nor violates the linearization assumptions. The vertical smoothing weighting parameter $s_Z$ is kept 0.5 after testing with range of the tomographic inversions of the tomographic inversion of values from 0 to 1. The number of non-linear iterations required to obtain the final model is 13, dropping the RMS traveltime misfits of the starting model (0.3 s) to the final model (0.047 s) by a factor of 6.4 having final $\chi^2$ of 1.04 (Table 1).

**Table 1**

First-arrival tomographic inversion parameters

| | |
|---|---|
| Shots | 10 |
| First-arrival picks | 1466 |
| Picking uncertainties (ms) | 50 |
| *nx* ä *nz* (finite-difference grid) | 241×21 |
| Node spacing (km) | 0.5 |
| Cell size, inverse grid (km) | 1.0 × 0.5 |
| Slowness cells | 2400 |
| Non-linear iterations | 13 |
| $T_{rms}$ (ms), $\chi^2$ (starting model) | 300, 27.6 |
| $T_{rms}$ (ms), $\chi^2$ (final model) | 47, 1.04 |

## Tomographic inversion results

The P-wave velocities of the Quaternary to Miocene sediments forming the recent alluvium cover vary from 1.8 to 2.0 km/s and the sediments gradually thicken from 0.5 to 1.0 km toward east of the profile. The basement velocity varies from 5.9 to 6.1 km/s throughout the delta and the exposed Chandikhol ridge toward west. The Bhubaneswar ridge is present in the east of the profile overlained by 1.0 km thick recent alluvium. The Gondwana graben lyin g between these two ridges has thick column (3.0 km) of Gondwana sediments surrounded by deep basinal faults. The tomographic inversion results, traveltime picks, fit of the tomographic model to the observed first-arrivals along with the final tomograph ic ray-tracing through the model are illustrated in Figures 3 and 4.

The upper 0.5-4.5 km of the tomographic velocity image obtained along the profile shows subhorizontal velocity contours (2.5-5.5 km/s) (Figure 3b). Significant lateral variations in the velocity model related to the Cuttack depression or Gondwana graben part of the delta is observed below this depth. The velocity interval 3.5-4.5 km/s is considered as due to the presence of upper-

Gondwana (UG) and lower-Gondwana (LG) sediments within the graben between two deep faults located at Cuttack and Kendrapara (Figure 1). A deepening of the basement having velocity contour of 6.0 km/s is observed inside the Gondwana graben between 25 km and 90 km model distance with maximum depth reached is 6.0 km near 60 km distance at the central part of the graben. The continuity of the 6.0 km/s contour is very much disturbed on either side of the graben at distances 25-45 km and 75-85 km, respectively, due to deep basinal faulting of the basement. These fault zones are also emplaced with volcanic intrusives considered as dykes having strong isolated velocity contours of 5.5 km/s at 30-40 km distance and sim ilar feature at 75-85 km. The 6.0 km/s contour gradually becomes shallow to 0.5 km in the west forming the Chandikhol ridge and attains 4.0 km depth in the east forming the Bhubaneswar ridge.

The perturbation of the final tomograph ic V p model with respect to the starting model is shown in Figure 3c. The length-scales of perturbations are a function of the resolution provided by the data, and reveal the real subsurface structure, which is not apparent in the tomographic model. The lateral and vertical extension of the two ridges and the Gondwana graben are well resolved in the perturbation plot with contours having positive velocity perturbations. The negative velocity perturbation zone indicate the extension of magmatic intrusives overlain by the Early Cretaceous Volcanic Province (ECVP) due to intense volcanism related to the rifting of the Indian Plate from Antarctica. The large velocity perturbations in this region are evident due to thick Gondwana sediments of average velocity 6.0 km/s related to the ridges. The velocity perturbation also indicates the spatial variation of the composition of different rock types in the delta along the profile.

There is very good match of the observed first-arrival traveltimes and the computed responses from the final tomographic model (Figure 4a). The misfits (differences of observed and computed data) are distributed uniformly around 0.0 s (Figure 4b) without much bias having RMS misfit of 47 ms. The maximum misfits of 70-100 ms are observed at distances of 50, 75, and 90-110 km along the profile due to small-scale strong lateral heterogeneities. The tomographic method can only resolve the overall, smooth velocity structure with the help of chosen grid cell sizes of 1.0 km × 0.5 km. Misinterpretation of the first-arrival phases, inconsistent picking of first-breaks on reverse data sections, and 3D effects may also contribute to the systematic misfits, although the traveltimes picked on reverse data sections in general match within the picking uncertainty of 50 ms. The first-arrival tomographic ray- tracing through the final model is shown in Figure 4c representing the nature of distribution of ray paths down to maximum 8 km depth.

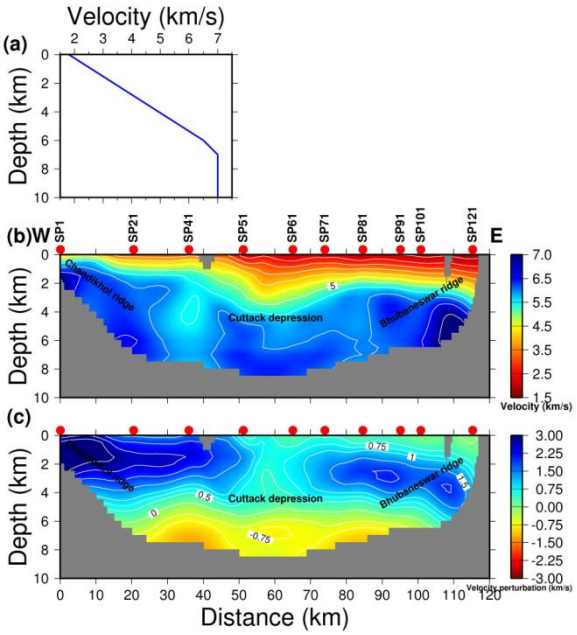


Figure 3. (a) Starting model for first-arrival tomography. (b) Final tomographic velocity model. (c) Perturbation of final tomographic velocity model with respect to the starting model. Red dots in each plot represent SPs with label and color scale with contours indicate the variation of model parameters in each plot. Regions not sampled by rays are left blank.

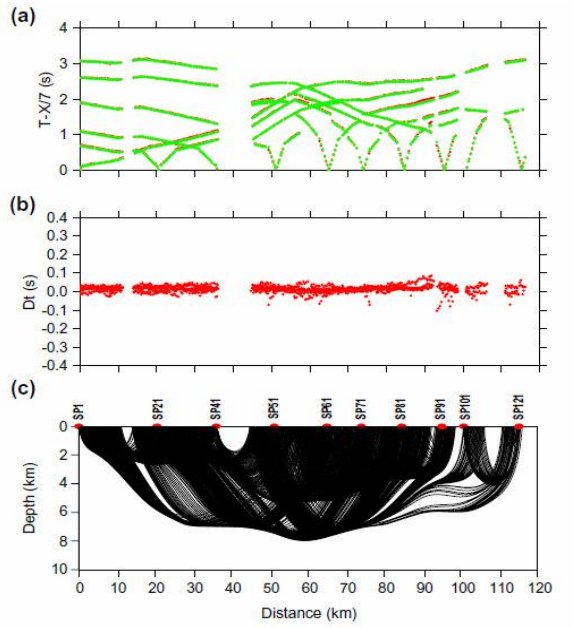


Figure 4. (a) Observed (red) and modeled first-arrival (green) traveltimes obtained from the final tomographic inversion, plotted in reduced scale with reduction velocity 7.0 km/ s. (b) Misfit (Dt) between the observed and first-arrival traveltimes. (c) First-arrival tomographic ray-tracing through the final model.

## Discussion

Previous studies in the delta are aimed at interpreting the Gondwana sequences and mainly focused on the structures such as the presence of horsts and grabens formed due to deep basinal faults of the basement. The deeper part of the delta has evidence of significant underplating and Moho upwarping because it has passed over the Kerguelen hot spot followed by Early Cretaceous volcanism (Behera et al., 2004). The ray-trace model derived using first-arrival traveltime data in the delta has constrained the thickness and velocities of the Gondwana sediments with velocity-interface layered structures above the basement (Figure 5). The tomographic image, however, delin eates smooth velocity variations (Figure 3b) and correlates well with the interface-depth structures derived by the ray-trace modeling superposed on it without much deviation (Figure 5). Because of the smooth and non-layered model parameterizations used in the refraction tomography, the velocity model obtained from this tomography approach can be used as a check on the long-wavelength structures and relative velocity variations in the ray-trace model.

This study documents the presence and extension of Gondwana sediments (UG and LG) within and outside of the graben, dyke intrusions due to intense volcanism during the Early Cretaceous period and imaged on either side of the graben as isolated high-velocity anomalies of 5.5 km/s. The volcanism has been spread to shallow depths through conduits formed due to basement faults and illustrated in the schematic cartoon representing the final tectonic model derived from the integrated interpretation of tomographic and ray-trace modeling in the delta (Figure 6). This can be related to ECVP of the delta due to intense magmatism followed by volcanic activity during the breakup and rifting of the Mahanadi Gondwana graben from its adjacent Lambert graben of Antarctica. These intrusives are transported from the deeper level due to extensional forces caused by plume head uplift and deposited in the upper crust as high-velocity (6.5 km/s) and high-density (2.8 g/cm$^3$) mafic magmatic materials (Behera et al., 2004). These magmatic activities have been related to the Kerguelen hot spot during the breakup and drifting of India and Antarctica (Mahoney et al., 1983; Kent, 1991; Storey, 1995). There are also many other magmatic activities reported in the eastern India correlated with the breakup of greater India and Antarctica with examples of both alkaline and tholeiitic magmatism of 130-120 Ma representing the Rajmahal, Bengal and Sylhet traps (Baksi, 1995), which are closely related to the Kerguelen hot spot. The thermal anomaly leading to a large-scale volcan ism and magmatic activity in the eastern India of Mahanadi delta as imaged from tomography may also be exhibited in the Lambert graben of Antarctica forming a major ECVP of both the continents because they were conjugate with each other before the breakup.

The tomographic method employed here relies only on the first-arrival traveltimes, which are picked w ith high precision by visual interpretation of seismic data (Figure 2). This is a powerful tool for imaging smooth and overall velocity distribution of the subsurface rocks, but inadequate to resolve detailed thin layering such as volcanic sills confined within the graben, whose position was constrained from the well data for ray-trace modeling by classifying the different phases based on the layer geometry and superimposed on the tomographic image to see the nature of correlation and amount of deviations arising out of these two modeling approaches adopted for

the same data set (Figure 5). The depth estimates and thickness variations found from the ray-trace modeling are consistent with the results obtained from the tomographic imaging and correlate well. The tomographic image (Figure 3c) provides information of the spatial extent of the horsts and grabens in terms of velocity heterogeneities showing compositional changes of different rock types like Gondwana sediments, granites/gneisses related to the basement, the presence of sub-basement magmatic intrusives, dykes and the nature of extension of volcanism in the delta to make the region geologically and tectonically significant (Figure 6).

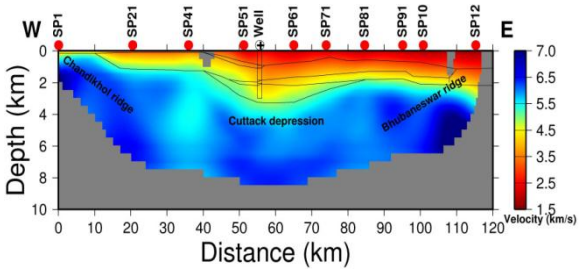


Figure 5. The final tomographic image superimposed with the interface-velocity structure derived from ray-trace modeling is shown for comparison. The improvement of the tomographic image is evident by delineating smooth velocity variations without having layers as shown in the ray-trace model. The basement is very deep in the Cuttack depression with the presence of thick Gondwana sediments. Very thin (100-200 m) high-velocity volcanics constrained from well data in the Gondwana graben for ray-trace modeling are not possible to image with tomography at this wavelength of seismic data.

The presence of Gondwana sediments within the graben is also important for hydrocarbon exploration in the delta. The thermal conditions due to volcanism and magmatism provide sufficient cooking temperatures for the generation of hydrocarbons with in the Gondwana sediments of the Mahanadi delta, which is considered as one of the major petroliferous basins of India. The thick (3.0 km) Gondwana sediments mainly comprise sandstones, siltstones and limestones within the graben provides sufficient P-T conditions for the maturation of hydrocarbon, which are considered as potential reservoir rocks. The main source rocks for hydrocarbon generation in the graben are the coal and shales of the Gondwana origin. The hydrocarbon generated are well confined within the graben because of deep basinal faults surrounding it and presence of basement ridges on either side of the graben (Figure 6) with suitable traps due to the presence of shales and volcanic sills.

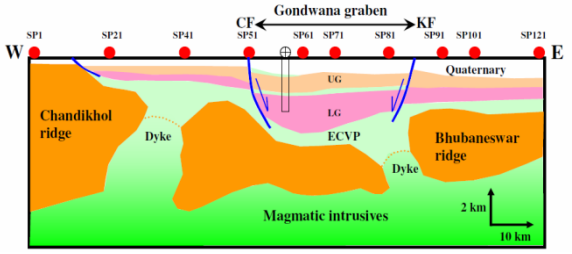


Figure 6. Schematic cartoon showing various tectonic features like horst-graben structure bounded by deep basinal faults Cuttack Fault (CF) and Kendrapara Fault (KF) forming the Gondwana graben as imaged from integrated interpretation of ray-trace modeling and tomographic imaging in the Mahanadi delta. The basement is overlained by thick high-velocity ECVP fed by dyke intrusions and magmatic intrusives through the deep basinal faults or conduits (dotted lines) due to intense E arly Cretaceous volcanic activity during the breakup of India from Antarctica.

## Conclusions

The following conclusions can be made from the tomographic inversion of first-arrival traveltimes along the said DSS profile in the Mahanadi delta: (1) The tomographic image shows the P-wave velocity variations and maximum thickness of the Gondwana sediments with the detailed configuration of the Gondwana graben having horsts on either side of the graben (Chandikhol ridge and Bhubaneswar ridge) along with sub-basement features in the delta. (2) The maximum thickness of the Gondwana sediments (UG) and (LG) imaged within the graben is 3.0 km with velocity variations from 3.5 km/s to 4.5 km/s. (3) The basement velocity varies from 5.9 km/s to 6.1 km/s with significant depression (6.0 km) below the Gondwana graben bounded by deep basinal faults. (4) The isolated high-velocity (5.5 km/s) anomalies imaged probably correspond to dyke intrusions on either side of the graben. These dykes are volcanic in nature and fed by the large volcanic edifice of ECVP having magmatic intrusives (6.5 km/s) lying below the basement. (5) The thickness and velocity variations of Gondwana sediments and basement configuration derived from ray-trace modeling of first-arrival seismic data correlates well with the tomographic image without much distortion. Hence, the final tectonic model derived by judicious integrated interpretation of ray-trace modeling and tomographic imaging is well

constrained. (6) Since the delta is sign ificant for hydrocarbon exploration, the thick Gondwana sediments imaged from the tomography may be suitable for finding potential hydrocarbon bearing zones in the Gondwana graben taking this as an input model for other geological and geophysical studies in the delta. (7) We determine basin sediment thickness and wave speeds, basement and sub-basement structure of the Mahanadi delta with relation to the magmatic edifice of the wide-spread volcanic activity that yielded dyke intrusions and basement uplift in a failed rift. We also briefly discuss possible implications of the derived tomographic image for future hydrocarbon exploration in the delta.

## Acknowledgements

We thank the Director NGRI (CSIR) for according permission to publish this paper. The author LB thanks DST, Govt. of India for awarding SERC-FAST Track Young Scientist Project (GAP-523-28 (LB)). Dr. Colin A. Zelt of Rice University, USA is gratefully acknowledged for RAYINVR and FAST codes.

## References

Anand, S. P., Erram, V. C. and Rajaram, M., 2002, Delineation of Mahanadi basin from ground magnetic survey; J. Geol. Soc. Ind., 60, 283-291.

Baksi, A. K., 1995, Petrogenesis and timing of volcanism in the Rajmahal flood basalt province, northeastern India; Chem. Geol., 21, 73-90.

Behera, L., 2003, Seismic imaging of Mahanadi delta and its tectonic significance; Ph.D. Thesis, Osmania University, Hyderabad, India.

Behera, L., Sain, K., Reddy, P. R., Rao, I. B. P. and Sarma, V. Y. N., 2002, Delineation of shallow structure and Gondwana graben in the Mahanadi delta, India, using forward modeling of first-arrival seismic data; J. Geodyn., 34, 127-139.

Behera, L., Sain, K. and Reddy, P. R., 2004, Evidence of underplating from seismic and gravity studies in the Mahanadi delta of eastern India and its tectonic significance; J. Geoph ys. Res., 109, B12311, doi: 10.1029/2003JB002764, 1-25.

Bharali, B., Rath, S. and Sarma, R., 1991, A brief review of Mahanadi delta and the deltaic sedim ents in Mahanadi basin : Quaternary deltas of India; Mem. Geol. Soc. Ind.,
22, 31-49.

Fedorov, L. V., Ravich, M. V. and Hofmann, J., 1982, Geologic comparison of southeastern peninsular India and Sri Lanka with a part of East Antarctica (Enderby Land, Mac Robertson Land, and Princess Elizabeth Land), In: Craddock, C. (Ed.); Antarctic Geoscience, Univ. Wis. Press, Madison, pp. 73-78.

Fuloria, R. C., 1994, Geology and hydrocarbon prospects of Mahanadi basin, India, In: Biswas, S. K. (Ed.); Second Seminar on Petroliferous Basins of India, vol. 3, Indian Petroleum, Dehradun, pp. 355-369.

Hofmann, J., 1996, Fragmente intragondwanischer rifte als werkzeug der Gondwana-rekonstruktion - Das beispiel des Lambert-Mahanadi-Riftes (Ostantarktika-Peninsular Indien); Neues Jarhb. Geol. Palaontol. Abh., 199, 33-48.

Hole, J. A., 1992, Nonlinear high -resolution three-dimensional seismic traveltime tomography; J. Geophys. Res., 97, 6553-6562.

Hole, J. A. and Zelt, B. C., 1995, Three-dimensional finite-difference reflection traveltimes; Geophys. J. Int., 121, 427 -434.

Kaila, K. L., Tewari, H. C. And Mall, D. M., 1987, Crustal structure and delineation of Gondwana sediments in the Mahanadi delta area, India, from deep seismic soundings; J. Geol. Soc. Ind., 29, 293-308.

Kent, R., 1991, Lithospheric uplift in eastern Gondwana: evidence for long lived mantle plume system?; Geology, 19, 19-23.

Lees, J. M. and Crosson, R. S., 1989, Tomographic inversion for three dimensional velocity structure at Mount St. Helens using earthquake data; J. Geophys. Res., 94, 5716-5728.

Mahoney, J. J., Macdougall, J. D., Lugmair, G. W. and Gopalan, K., 1983, Kerguelen hot spot source for Rajmahal traps and Ninety East ridge; Nature, 302, 385-389.

Mishra, D. C., Chandra Sekhar D. V., Venkata Raju, D. C. And Vijay Kumar, V., 1999, Crustal structure based on gravity-magnetic modeling constrained from seismic studies under Lambert rift, Antarctica and Godavari and Mahanadi rifts, India and their interrelationship; Earth Planet Sci. Lett., 172, 287-300.

Rao, G. N., 1993, Geology and hydrocarbon prospects of east coast sedimentary basins of India with special reference to Krishna-Godavari basin; J. Geol. Soc., Ind., 41, 444-454.

Sastri, V. V., Raju, A. T. R., Sinha, R. N. and Venkatachala, B. S., 1974, Evolution of Mesozoic sedimentary basins on the east coast of India; APEA J., 14, 29-41.

Storey, B. C., 1995, The role of mantle plumes in continental breakup, case histories from Gondwanaland; Nature, 377, 301-308.

Vidale, J. E., 1988, Fin ite-difference calculations of traveltimes; Bull. Seismol. Soc. Am., 78, 2062-2076.

Zelt, C. A. and Barton, P. J., 1998, Three-dimensional seismic refraction tomography: a comparison of two methods applied to data from Faroe Basin; J. Geophys. Res., 103, 7187-7210.

Zelt, C. A. and Smith, R. B., 1992, Seismic traveltime inversion for 2-D crustal velocity structure; Geophys. J. Int., 108, 16-34.